Stability of a dome-shape liquid film for conditions when it flows around a plate

R A Dekhtyar[1,2], E Yu Slesareva[1], and V V Ovchinnikov[1]

[1]SB RAS, Kutateladze Institute of Thermophysics, 630090 Novosibirsk, Russia

Corresponding author: dekhtyar@itp.nsc.ru

Abstract. The experimental research of hydrodynamic stability of a dome-shape film of liquid for the conditions, when it flows around a thin plate has been carried out. Experiments have been executed for a case of Savart "water bell". An axisymmetrical film has been formed by the impact of a liquid jet with the width of 10 mm on a solid disc with the diameter of 14.5 mm. The width of the thin plate, streamlined by a dome-shape water film, was varied from 0.05 to 3.5 mm. The wide side of the plate was located at two angles relative to the direction of the flow velocity vector in a film: along and across, at various distances from the disc. Stability of the "water bell" surface has been considered and general stability criterion showing its sensitivity to the angle of plate orientation has been derived. The critical Weber number, above which the discontinuity of bell surface appears, and threshold value of the Weber number, below which it coalescences, have been defined. It was shown, that the critical and threshold Weber numbers depend on the Reynolds number.

1. Introduction

The use of a liquid film in heat exchangers (condensers, absorbers, distillation columns, etc.) is important for studying such flow. The structure of the thin liquid film flow influences significantly the local and average characteristics of heat and mass transfer. It is known that intensification of heat and mass transfer in the case of developed wave surface occurs both because of an increase in the surface of heat and mass transfer, and due to a change in the velocity profile of the liquid film [1, 2]. One of the forms of the liquid film is the dome-shaped film. Such films are formed, when the liquid flow impinges a solid disk. The first investigation of the dome-shaped liquid films, the so-called «water bells», has been published in 1833 by Felix Savart [3]. In [4, 5], the models of a «water bell» are submitted. The liquid film velocity U depending on distance Y from a disk surface is presented by dependence [4, 5]

$$U = \sqrt[2]{U_0^2 + 2 \cdot g \cdot Y}\ , \qquad (1)$$

where g is gravity acceleration, U_0 is velocity on the brink of a disk. The liquid film thickness δ at section Y is calculated in following form

$$\delta = \frac{Q}{2\pi \cdot R \cdot U}\ , \qquad (2)$$

here Q is the volumetric rate of liquid flow, R is radius of a «water bell» profile in the cross-section at altitude Y.

In [6], the flow film is checked experimentally by puncturing the bell. In the period immediately following the puncture, when the pressurized air has not yet escaped from the cavity through the

growing hole, the bell shape remains globally unchanged. One then sees that, a) the border of the hole, disturbed upstream, is entrained by the flow as expected for usual supercritical liquid; (b) the border of the hole, disturbed downstream, recedes against the flow, as it corresponds to the subcritical flow. To generate the developed wave surface, the aggregated thin rods are used. At interaction of the dome-shaped film flow with a rod, destruction of the liquid film surface can occur. It is demonstrated in figure 1, the flow regime changes, when rod assemblage is shifted up by 20 mm for constant water flow rate.

The rod diameter and water flow rate are insufficient for determination of the flow regime. It is required to define the additional criteria, allowing us to predict the flow regime considering the rod position relative to the «water bell» surface. The problem can be simplified if we observe the conditions of stability for a thin plate with width ζ. The purpose of this work is obtaining and analysis of data on hydrodynamic stability of a dome-shaped liquid film in the flow around a thin plate.

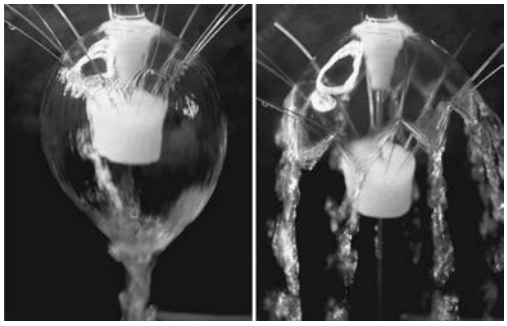

Figure 1. Influence of position of 12 aggregated thin rods relative to the «water bell» surface on the flow regime. On the left, there is a continuous film flow, on the right, it is broken. Diameter of rods is 0.35 mm, flow rate is Q = 55 ml/s, U_0 = 0.74 m/s.

2. A measurement procedure

Experiments with a «water bell», formed at a leak-in of a water jet on a disk with the diameter of 14.5 mm were carried out. The jet was formed at the exit of a brass tube with the inner diameter of 10 mm at the distances from 5 to 60 mm between a tube edge and disk surface. The flow rate was measured by the pressure drop on the calibrated glass tube of 400-mm length and 9.5-mm diameter. Flow rate was calibrated by measuring the rate of the weight change in the filled volume. Calibrating accuracy was 0.3 ml/s. The flow patterns were recorded by a digital camera with the speed of 300 fps. The study the effect of the plate width on the liquid film flow, wedge-shaped plate from stainless steel of 0.1-mm thickness was used, the plate width was changed from 0.05 to 3.5 mm at the length of 34.5 mm. Size ζ was determined in the area of plate surface intersection with the liquid film. In experiments, ζ was determined by length $\mathcal{L}$, obtained at video frame processing (figure 2). In experiments, the plate wide side was mounted at two angles relative to the flow velocity vector; in the film, it was located along and across at a various distance from the disc. By means of a microscrew, the plate was moved along the normal to the film surface and this allowed precise determination of size ζ at the moment of destructing or rebuilding the liquid film surface to the dome shape.

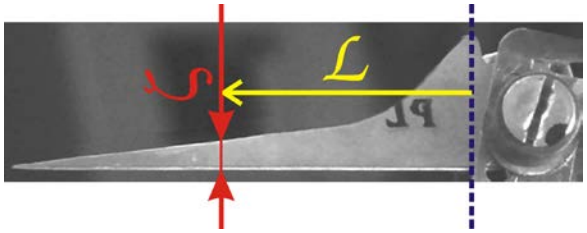

Figure 2. The scheme of determination of the value of the plate wide side ζ by measuring length $\mathcal{L}$. ζ = $f(\mathcal{L})$.

Values U and δ are computed by ‘dependences (1) and (2)’, accordingly. Processing the video frames of a «water bells» has shown that dependence of radius profile R on location Y can be presented by smooth functions in the following form:

$$R = A \cdot Y^a \cdot \exp\left[\left(\frac{Y - C}{B}\right)^b\right] \qquad (3)$$

Examples of comparisons of the «water bell» shapes with calculation by ‘dependence (3)’ are presented in figure 3 for various flow rates Q. As is follows from figure 3, the dependence describes the shape film well, if it does not consider the ripples on the surface. Thus, using ‘equations (1-3)’, for any point of the dome-shape film, it is possible to calculate liquid velocity U and film thickness δ. These values are necessary for computation of the dimensionless parameters, which define the stability conditions of the dome-shape film.

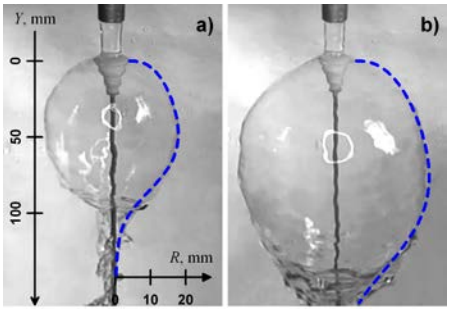

Figure 3. Video frames of the flow of dome-shaped liquid film for different flow rates Q, **a**) 52 ml/s; **b**) 73 ml/s. Dashed line is calculation R (Y) by ‘dependence (3)’.
For sizes in "mm", the value of parameters A, a, B, b in ‘dependence (3)’ is:
a) A = 3.9; a = 0.5; B = 132; b = 12; C = -50.
b) A = 5.9; a = 0.5; B = 164; b = 8; C = -34.

3. Discussion of results

Hydrodynamic stability of a dome-shape liquid film was studied experimentally for the conditions, when it flows around a thin rod and thin plate, and when a water droplet falls on the film surface. The experiment has been executed for the case of Savart "water bell".

When a water droplet falls on the film surface, the wavetrain from the centre at the droplet fall point is formed. This centre is displaced downwards along the flow. If the wave amplitude reaches the magnitude commensurable with the film thickness, a hole is formed the wavetrain centre on the surface. This hole expands with approximately constant velocity and displaces simultaneously downstream. However, the complete destruction of the bell does not happen, or the hole is carried away from a water bell, or the upper edge of the hole moves in the direction of the disk, where the boundary line stops, and reverse motion of the hole boundary line occurs, and this initiates the rebuilding of the film surface. The video frames of the wave and hole on the surface after water droplet fall on the dome-shape film are presented in figure 4. In this case, the droplet falls on the upper part of the bell, the hole on the surface appears through 73 ms after collision in a medial part of the bell. The average velocity of hole expansion is 2 m/s.

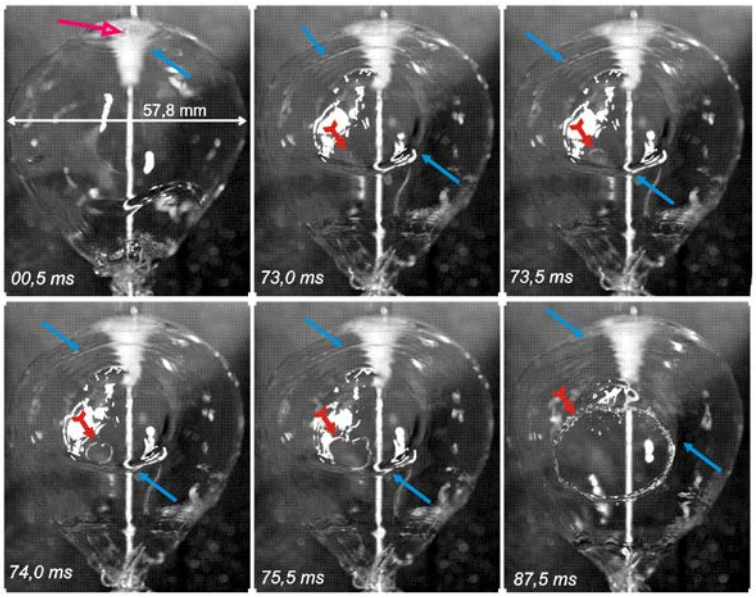

Figure 4. Video frames of wave (blue arrow) and hole (red sign) development on a surface after water droplet fall (red arrow, 0.5 ms) on a dome-shape film. Flow rate is Q = 48 ml/s; U_0 = 0.73 m/s. Video speed is 5000 fps.

The experimental research showed stability of the "water bell" surface and derived the general stability criterion showing its sensitivity to the angle of location on the plate wide side. Plate width ζ

has critical value ζ_C above which the surface of a dome-shape liquid film is broken below the plate and threshold value ζ_T below which it coalesces.

Three samples of video frames are shown in Figure 5 at different plate widths, total water flow rate of 73 ml/s and initial velocity of 1.2 m/s. For this case, the plate wide side is disposed along the flow velocity vector. It is possible to see the different conditions on the liquid surface, while the dome-shape liquid film flows around a plate. On the left of the picture, the wavetrain (wave regime) is generated in front and behind the plate for case, when $\zeta < \zeta_C$. Discontinuity of the liquid film (discontinuity regime) occurs below the plate in the picture centre for the case, when $\zeta = \zeta_C$. Coalescence of the liquid film (coalescence regime) is observed on the right of the picture for case, when $\zeta < \zeta_T$.

Figure 5. Patterns of the dome-shaped film, when the plate wide side is located along the flow velocity vector. On the left - wave regime, in the centre - discontinuity, on the right - coalescence. Flow rate is Q = 73 ml/s; U_0 = 1.2 m/s.

Using the obtained data on velocity U, film thickness δ, plate width ζ, dimensionless criteria have been counted at the moment of destructing or rebuilding of the liquid film on the «water bell» surface. These are Reynolds number $\mathrm{Re}_\delta = \frac{U \cdot \delta}{\nu}$ and Weber number $\mathrm{We}_\zeta = \frac{\rho \cdot U^2 \cdot \zeta}{\sigma}$, where ν is kinematic viscosity of liquid, ρ is density of liquid, σ is surface tension. Two types of conditions on the liquid surface for dimensionless parameters We_ζ vs. Re_δ are presented in figure 6. The first type is when $\zeta = \zeta_C$, the second type is when $\zeta = \zeta_T$. It is possible to see that for the case, when the plate wide side is disposed along the flow velocity vector, coalescence of the film surface occurs at the widths less, than that corresponding to discontinuity.

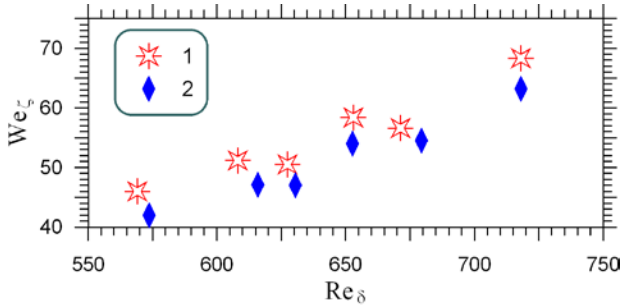

Figure 6. The flow pattern map as function We_ζ of Re_δ for the case when the plate wide side is located along the flow velocity vector. 1 - discontinuity of a liquid film below a plate; 2 – coalescence of a liquid film below a plate.

Like in figure 5, three samples of the video frames are shown in Figure 7 at different plate widths, under the total water flow rate of 52 ml/s and initial velocity of 0.94 m/s. For this case, the wide side of the plate is disposed across the flow velocity vector. The wave regime, when $\zeta < \zeta_C$, is shown on the left picture; discontinuity regime, when $\zeta = \zeta_C$, is in the picture centre; and coalescence regime, when $\zeta < \zeta_T$, is on right of the picture. The flow pattern map as We_ζ function of Re_δ for the case, when the plate wide side is disposed across the flow velocity vector, is presented in figure 8. It is possible to see that for the case, when the plate wide side is disposed across the flow velocity vector, film surface discontinuity occurs if the width is much smaller, than that at coalescence. Line 3 indicates that in this case, film surface coalescence occurs, if plate width ζ is close to film thickness δ.

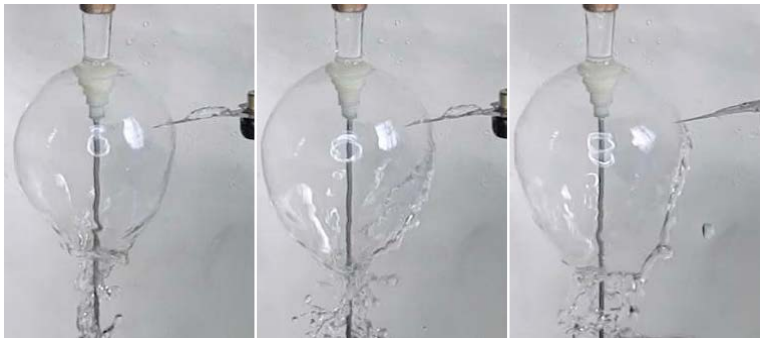

Figure 7. Patterns of the dome-shaped film, when the plate wide side is located across the flow velocity vector. On the left - wave regime, in the centre - discontinuity, on the right - coalescence. Flow rate is Q = 52 ml/s; U_0 = 0.94 m/s.

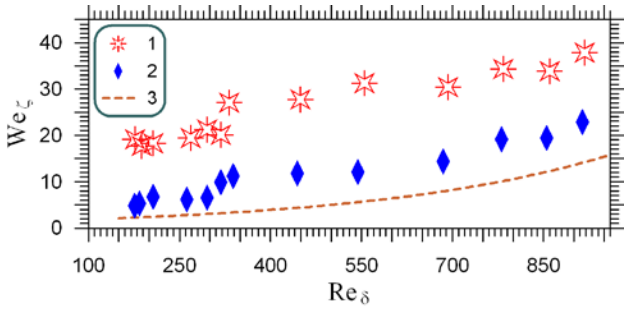

Figure 8. The flow pattern map as function We_ζ of Re_δ for the case, when the plate wide side is located across the flow velocity vector. 1 - discontinuity of a liquid film below a plate; 2 - coalescence of a liquid film below a plate; 3 - Weber number We_ζ at $\zeta = \delta$.

Thus, the experimental research shows that the critical and threshold Weber numbers depend on the Reynolds number at the inter-section point. If rod diameter d is less than local film thickness δ, then the flow without separation is quite possible under the conditions, when the dome-shape film flows around the rod.

4. Conclusion

The experimental research shows that rod diameter d, plate size ζ and water flow rate Q are insufficient for determination of the flow regime. Stability of the dome-shape film surface has been considered and general stability criterion showing its sensitivity to the angle of plate orientation has been derived. If the plate wide side is oriented across the flow velocity vector, discontinuity of the film surface occurs, when the plate width is much smaller than that at coalescence. If the plate wide side is oriented along the flow velocity vector, coalescence of the film surface occurs, when the plate width is slightly less than that at discontinuity. We have determined the critical Weber number above which the discontinuity of bell surface appears and the threshold Weber number below which it coalescences. It is shown that the threshold and critical local Weber numbers depend on the local Reynolds number at the inter-section line of the bell with the plate.

This work was supported by the Russian Science Foundation (project no. 15-19-10025).

References

[1] Alekseenko S V, Nakoryakov V E, Pocusaev B G 1994 *Wave Flow of Liquid Films* (New York: Begell house)
[2] Nakoryakov V E, Misyura S Y and Elistratov S L 2013 *J. Engin. Therm.*, **22(1)**, 1
[3] Savart F 1833 *Ann. De Chim.*, **54** 56
[4] Taylor G 1959 *Proc. R. Soc. London A*, **253(13)** 289
[5] Parlange J Y 1967 *J. Fluid Mech.* **29(2)** 361
[6] Lhuissier H and Villermaux E 2012 *J. Fluid Mech.* **693** 508